J Fluoresc (2009) 19:857–866
DOI 10.1007/s10895-009-0483-x

ORIGINAL PAPER

Synthesis, Characterization, DNA-Binding and Antiproliferative Activity of Nd(III) Complexes With N-(Nitrogen Heterocyclic) Norcantharidin Acylamide Acid

Wen-Zhong Zhu · Qiu-Yue Lin · Mei Lu · Rui-Ding Hu · Xiao-Liang Zheng · Jian-Ping Cheng · Yun-Yun Wang

Received: 8 November 2008 / Accepted: 27 March 2009 / Published online: 25 April 2009

Abstract Three novel complexes $[Nd(L)(NO_3)(H_2O)_2]\cdot NO_3\cdot 2H_2O$ (HL^1 = N-pyrimidine norcantharidin acylamide acid, $C_{12}H_{13}N_3O_4$; HL^2=N-pyridine norcantharidin acylamide acid, $C_{13}H_{14}N_2O_4$; HL^3 = N-phenyl norcantharidin acylamide acid, $C_{14}H_{15}NO_4$) were synthesized. HL^1, HL^2 and HL^3 are the ligand of complex(**1**), complex(**2**) and complex(**3**), respectively. Their structures were characterized by elemental analysis, conductivity measurement, infrared spectra and thermogravimetric analysis. The DNA-binding properties of the complexes have been investigated by fluorescence spectroscopy and viscosity measurements. The results suggest that the complexes can bind to DNA by partial intercalation. The liner Stern-Volmer quenching constant K_{sq} values are 3.3(±0.21)(**1**), 1.7(±0.19)(**2**) and 0.9 (±0.04)(**3**), respectively. Complex (**1**) and (**2**) have been found to cleave pBR322 plasmid DNA at physiological pH and temperature. The test of antiproliferation activity indicates that complex(**1**) has strong antiproliferative ability against the SMMC7721 (IC_{50}=131.7±23.4 μmol·L^{-1}) and A549 (IC_{50}=128.4±19.9 μmol·L^{-1}) cell lines. The inhibition rates of complex(**2**) (IC_{50}=86.3±11.3 μmol·L^{-1}) are much higher than that of NCTD (IC_{50}=115.5±9.5 μmol·L^{-1}) and HL^2 (111.0±5.7 μmol·L^{-1}) against SMMC7721 cell lines.

Keywords Norcantharidin · Nd(III) complexes · Pyrimidine · Pyridine · DNA binding · Antiproliferative activity

W.-Z. Zhu · Q.-Y. Lin · R.-D. Hu (✉) · J.-P. Cheng · Y.-Y. Wang
Zhejiang Key Laboratory for Reaction Chemistry on Solid Surfaces,
Zhejiang Normal University,
Jinhua 321004, China
e-mail: huruiding@zjnu.cn

W.-Z. Zhu · Q.-Y. Lin · M. Lu · R.-D. Hu · J.-P. Cheng · Y.-Y. Wang
College of Chemical and Life Science,
Zhejiang Normal University,
Jinhua 321004, China

X.-L. Zheng
Institute of Matria Medica,
Zhejiang Academy of Medical Sciences,
Hangzhou 310013, China

Introduction

Norcantharidin have attracted much attention, not only for its anticancer activity and stimulatory to the bone marrow [1], but also for its weak nephrotoxicity [2]. Many derivatives of norcantharidin were synthesized and some of them have good anti-tumor activity in vitro [3, 4].

The lanthanide metal complexes also have many noticeable bioactivities [5]. One of the most studied applications is usage of the lanthanide complexes or small molecule complexes to address DNA/RNA by non-covalent binding and/or cleavage [6]. In a recent report, the synthesis of the complexes of norcantharidin [7, 8] plays an important role in researching of high anti-tumor activity of the drug.

To improve the action of drugs with DNA in cells and understand the mechanism of action at the molecular level, we have synthesized norcantharidin acylamide acids HL(HL^1 = N-pyrimidine norcantharidin acylamide acid; HL^2 = N-pyridine norcantharidin acylamide acid; HL^3 = N-phenyl norcantharidin acylamide acid) and three novel complexes $[Nd(L)(NO_3)(H_2O)_2]\cdot NO_3\cdot 2H_2O$. The interaction of complexes with calf thymus DNA was investigated by fluorescence spectroscopy and viscosity measurements. The DNA

cleavage experiments induced by the compounds were also carried out . Furthermore, the antiproliferative activities of the compounds toward SMMC7721 and A549 cell lines in vitro were also evaluated with MTT cell viability assay.

Experimental

Materials and instruments

Norcantharidin(NCTD,$C_8H_8O_4$) was obtained from Suzhou Sunray Pharmaceutical Co. 2-aminopyrimidine, 2-aminopyridine and aniline were purchased from Sinopharm Chemical Reagent Co. Nd(III) nitrates were obtained by neutralizing Nd_2O_3(Sinopharm Chemical Reagent Co.; at least 99.9% purity) with nitric acid, followed by evaporation to near dryness. Aniline and THF (Analytical Reagent) were distilled before use. Other chemical reagents for synthesizing the title compounds were all purchased commercially and used without further purification. MTT(3-[4,5-dimethylthiazol -2-yl]-2,5-diphenyl tetrazolium bromide) was purchased from the Sigma Company.

Calf thymus DNA (ct-DNA, Huamei Co.) was dissolved in 50 mmol·L^{-1} NaCl, 5 mmol·L^{-1} Tris-HCl (pH 7.4). The ratio of the absorbance A_{260}/A_{280} was checked to be 1.80–1.90, indicating that the DNA was sufficiently free of protein. Plasmid DNA (pBR322) purchased from Shanghai Biologic Engineering Co. was diluted to 25 μg·mL^{-1}. Double-distilled water was used to prepare buffer solutions. Human hepatoblastoma cells (SMMC7721) and human lung cancer cells (A549) were purchased from Shanghai Institute of Cell Bank, Shanghai, China.

Elemental analyses for carbon, hydrogen, nitrogen were carried on a Vario EL III elemental analyzer. The molar conductance values were determined in DMF on an Orion 150 Aplus conductance meter. The infrared spectra were obtained using a NEXUS-670 FT-IR spectrometer in the 4000–400 cm^{-1} regions, using KBr pellets. Ultraviolet-visible spectra were obtained on a UV-2501PC spectrophotometer. ^{1}H NMR was run on a Brucker Avance-400 (400MH) spectrometer using trimethylsilyl (TMS) as standard internal reference. The thermal behavior was monitored on a TGA/SDTA851^e thermo gravimetric and differential thermal analyzer. Fluorescence emission spectra were recorded with a Perkin-Elmer LS-55 spectrofluorometer. Agarose gel electrophoresis was performed on Power-Pac Basic electrophoresis apparatus (BIO-RAD). Gel image formation were obtained on UNIVERSAL HOOD 11-S.N. (BIO-RAD Laboratories). Sheldon CO_2 culture box and East-China Electronic tube Factory DG3022A ELISA instruments were used to perform antiproliferative activity.

Synthesis

Preparation of norcantharidin acylamide acids (HL)

Three ligands (HL) was synthesized by similar method [9]. In 15 mL THF, norcantharidin (4.12 g, 25 mmol) was dissolved, wherein aromatic amines (2-aminopyrimidine, 2-aminopyridine or aniline) (25 mmol) solution in THF was dropwisely added with stirring. The mixture was reacted for 2 h at room temperature and precipitate was obtained. The precipitate was filtered. Then the compound was recrystallized by 95% ethanol, and dried for 2 h in a vacuum. The preparation routes of the ligands are outlined in Fig. 1. The structures were characterized by elemental analysis, IR, UV and ^{1}H NMR. Anal. Calcd. for HL^1 (N-pyrimidine norcantharidin acylamide acid, $C_{12}H_{13}N_3O_4$): C, 54.75; H, 4.98; N, 15.96. Found: C, 53.01; H, 5.39; N, 15.11. IR (KBr pellet, cm^{-1}): ν(N-H) 3339 (s); $\nu_{(C=O)}$(COOH) 1703 (s); $\nu_{(C=O)}$(CONH) 1669 (s); ν(pyrimidine ring, C = N) 1627(s); ν(C-O-C) 1170(s). UV-Vis: 293.5 nm, 220.5 nm. ^{1}H NMR (DMSO-d_6), δ (ppm): 6.52–6.56(m, 3H, Ar-H); 4.66–4.67(m, 2H, C_1C_4-H); 2.90(d, 2H, C_2C_3-H); 1.48–1.56(m, 4H, C_5C_6-H). Anal. Calcd. for HL^2 (N-pyridine norcantharidin acylamide acid, $C_{13}H_{14}N_2O_4$): C, 59.54; H, 5.38; N, 10.68. Found: C, 59.60; H, 5.43; N, 9.90. IR (KBr pellet, cm^{-1}): ν(N-H) 3316 (s); $\nu_{(C=O)}$(COOH) 1714(s); $\nu_{(C=O)}$(CONH) 1662 (s); ν(pyridine ring, C = N) 1622(s); ν(C-O-C) 1172(s). UV-Vis: 299.4 nm, 229.6 nm. ^{1}H NMR

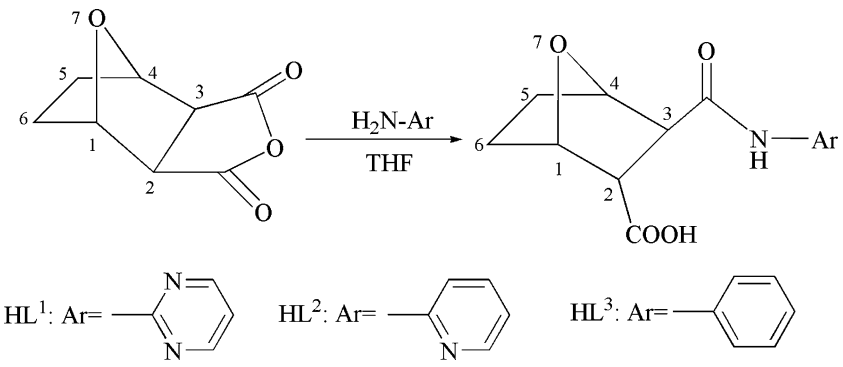

Fig. 1 The synthesis route of HL^1, HL^2 and HL^3

(DMSO-d), δ (ppm): 6.42–7.88(m, 4H, Ar-H), 4.64–4.65 (m, 2H, C_1C_4-H), 2.90(d, 2H, C_2C_3-H), 1.47–1.55(m, 4H, C_5C_6-H). Anal. Calcd. for HL^3 (N-phenyl norcantharidin acylamide acid, $C_{14}H_{15}NO_4$): C, 64.36;H, 5.78; N, 5.36. Found: C, 64.77; H, 5.98; N, 5.09. IR (KBr pellet, cm^{-1}): ν(N-H) 3302 (s); $\nu_{(C=O)}$(COOH) 1720(s); $\nu_{(C=O)}$(CONH) 1681 (s); ν(benzene ring, C = C) 1601(s); ν(C-O-C) 1170 (s). UV-Vis: 240.8 nm. ^{1}H NMR (DMSO-d), δ (ppm): 11.96(s, 1H, COOH); 9.65(s, 1H, NH); 6.99–7.53 (m, 5H, Ar-H); 4.62–4.79(m, 2H, C_1C_4-H), 2.90(d, 2H, C_2C_3-H), 1.49–1.61(m, 4H, C_5C_6-H).

Synthesis of the complexes

In 50 mL round-bottomed flask, HL^1 (0.262 g, 1 mmol) was dissolved in mixed solvents of ethanol and chloroform (1:1, v/v) (20 mL). Then the solution of Nd $(NO_3)_3{\cdot}6H_2O$ (0.438 g, 1 mmol) in ethanol (5 mL) was dropwisely added with stirring. Immediately there was purple precipitate in the solution. After stirring for 2 h at room temperature, the precipitate of complex (**1**) was filtered, washed with 95% ethanol, and then dried in vacuums. In similar way, complexes (**2**) and (**3**) were synthesized with HL^2 and HL^3 respectively.

Complex(**1**): yield 65%. Anal. Calcd for $C_{12}H_{21}N_5O_{14}Nd$: C, 23.88; H, 3.51; N, 11.60. Found: C, 24.48; H, 3.44; N, 11.23. IR (KBr pellet, cm^{-1}): $\nu_{(C=O)}$(CONH) 1683(s); $\nu_{as}(COO^-)$ 1576(s); $\nu_s(COO^-)$ 1449(s); ν(C-O-C) 1178(m); ν(pyrimidine ring, C = N) 1626(s); $\nu(NO_3^-)$1384 (s); $\nu_1(NO_3^-)$ 1495(m); $\nu_2(NO_3^-)$ 1043(m); $\nu_3(NO_3^-)$ 820 (m); $\nu_4(NO_3^-)$ 1299 (m). UV-Vis: 295.4 nm. Λm (DMF): 79 $S{\cdot}cm^2{\cdot}\ mol^{-1}$. Complex (**2**): yield 58%. Anal. Calcd for $C_{13}H_{22}N_4O_{14}Nd$: C, 25.91; H, 3.68; N, 9.30. Found: C, 26.49; H, 3.24; N, 9.14. IR (KBr pellet, cm^{-1}): $\nu_{(C=O)}$(CONH) 1669(s); $\nu_{as}(COO^-)$ 1580(s); $\nu_s(COO^-)$ 1452(s); ν(C-O-C) 1176(m); ν(pyridine ring, C = N) 1621 (s); $\nu(NO_3^-)$ 1384 (s); $\nu_1(NO_3^-)$ 1493(m); $\nu_2(NO_3^-)$ 1041 (m); $\nu_3(NO_3^-)$ 819 (m); $\nu_4(NO_3^-)$ 1308 (m). UV-Vis: 293.4 nm. Λm (DMF): 83 $S{\cdot}cm^2{\cdot}\ mol^{-1}$. Complex (**3**): yield 87%. Anal. calcd for $C_{14}H_{23}N_3O_{14}Nd$: C, 27.95; H, 3.85; N, 6.98. Found: C, 27.70; H, 4.24; N, 6.67. IR (KBr pellet, cm^{-1}): $\nu_{(C=O)}$(CONH) 1626(s); $\nu_{as}(COO^-)$ 1565(s); $\nu_s(COO^-)$ 1448(s); ν(C-O-C) 1176(m); ν(benzene ring, C = C) 1600(s); $\nu(NO_3^-)$ 1384 (s); $\nu_1(NO_3^-)$ 1494(m); $\nu_2(NO_3^-)$ 1031(m); $\nu_3(NO_3^-)$ 817(m); $\nu_4(NO_3^-)$ 1315(m). UV-Vis: 242.4 nm. Λm (DMF): 67 $S{\cdot}cm^2{\cdot}\ mol^{-1}$.

DNA binding and cleavage experiments

Fluorescence spectra

Fluorescence quenching experiments of the complexes were carried out by adding $3.74\times10^{-4}mol{\cdot}L^{-1}$ ct-DNA solution at different concentrations (0–54 $\mu mol{\cdot}L^{-1}$) to the samples containing 20 $\mu mol{\cdot}L^{-1}$ complexes solution and Tris-HCl buffer (pH 7.4). After incubation for 4 h at 4 °C, all the samples were excited at 280 nm and emission was observed between 300 and 500 nm.

Fluorescence quenching experiments of EB-DNA were carried out by adding complexes or HL solution(0.2 $mmol{\cdot}L^{-1}$) to the samples containing 50 $\mu mol{\cdot}L^{-1}$ EB, 74 $\mu mol{\cdot}L^{-1}$ DNA and Tris-HCl buffer (pH 7.4) at different concentrations (0–89 $\mu mol{\cdot}L^{-1}$). All the samples were excited at 525 nm and emission was recorded at 530–700 nm.

Viscosity

Viscosity experiments were conducted on an Ubbdlodhe viscometer, immersed in a thermostatic water-bath maintained at 30 °C. The complex was introduced into a DNA solution ($3.74\times10^{-4}mol{\cdot}L^{-1}$) by microsyringe. Flow time was measured by a digital stopwatch. The average values of three replicated measurements were used to evaluate the viscosity of the samples. Data were represented as $(\eta/\eta_0)^{1/3}$ versus the ratio of the concentration of the compound to DNA, where η and η_0 were the viscosity of DNA in the presence and absence of complexes, respectively. Viscosity were calculated from the observed flow time of DNA solution in the presence of complexes (t), corrected from the flow time of buffer alone (t_0), $\eta = (t - t_0) / t_0$.

Interaction with pBR322 plasmid DNA

The compounds were incubated with the pBR322 plasmid DNA in order to understand whether any interaction occurred. The incubation time lasted for 3 h at 37 °C until 0.25% bromophenol blue and 1 mmol L^{-1} EDTA were added. The DNA cleavage products were subjected to electrophoresis on 1.0% agarose gel containing 0.5 $\mu g\ mL^{-1}$ ethidium bromides. The gels were run at 110 V for 1.2 h in Tris-acetic acid-ethylenediaminetetraacetic acid (TAE) buffer and the bands were photographed.

Antiproliferative activity evaluation [10]

The antiproliferative activity of the compounds was evaluated by using human hepatoma cells SMMC7721 and human lung cancer cells A549. The anti-proliferatives activity was measured by the MTT assay. The cancer cells were incubated with 10% fetal serum, 40 $U{\cdot}mL^{-1}$ gentamicin DMEM (Dulbecco's Modified Eagle Medium, high glucose) nutrient solutions in culture boxes and in a humidified atmosphere with 5% CO_2 at 37 °C. Compounds were dissolved in DMSO as 100 $mmol{\cdot}L^{-1}$ stock solutions and diluted with culture medium before used. Growth cells in the exponential phase were assayed in 96-well plates by adding 100 μL stock solution directly to culture wells. After the cells were seeded

for 24 h, the complexes, HL or NCTD were added. Then the cells were incubated for 72 h, followed by adding 100 μL MTT (1 mg·mL^{-1}, dissolved in DMEM nutrient solution) into each well for 4 h at 37°C. Later, the liquid in each well was abandoned and then 150 μL acidifying isopropanol (containing 0.04 mol·L^{-1} HCl) was added. The mixture was placed in a dark area for 30 min. The inhibition rate and IC_{50} were calculated.

Result and discussion

Characterization of the complexes

Elemental analysis and conductivity measurement

All of complexes are soluble in DMF and DMSO, insoluble in ether, ethanol, chloroform and benzene, and can be kept in air for a long time. The molar conductance values in 1×10^{-3}mol· L^{-1} DMF are around 67–83 Scm^2 ·mol^{-1}, which suggests that they are 1:1 type electrolytes [11]. The elemental analyses and molar conductance data show that the formulae of the complexes are $[Nd(L^1)(NO_3)(H_2O)_2]\cdot NO_3\cdot 2H_2O$(**1**), $[Nd(L^2)(NO_3)(H_2O)_2]\cdot NO_3\cdot 2H_2O$ (**2**) and $[Nd(L^3)(NO_3)(H_2O)_2]\cdot NO_3\cdot 2H_2O$(**3**).

Infrared spectra

The mode of binding of the ligands to Nd(III) can been elucidated by compared the IR spectra of the complexes with that of the free ligands (HL). It can be found that the characteristic vibrational bands of all complexes are similar. All the spectra are characterized by vibrational bands mainly due to the NH, C = O (CONH), COOH, C-O-C and C = N (aromatic cycle).

The ν_{NH} band of the HL^1, HL^2 and HL^3 appears at 3339, 3316 and 3302 cm^{-1}, respectively. But this band was covered by $\nu_{OH}(H_2O)$ vibrations band of crystal water in complexes. The ν_{CO}(CONH) for the HL^1, HL^2 and HL^3 appears at 1669, 1662 and 1681 cm^{-1}, but for the complex (**1**), (**2**) and (**3**), the peak shifts to 1683,1669 and 1626 cm^{-1}, respectively. The shifts demonstrate that the oxygen of carbonyl has formed a coordinative bond with the Nd(III) ion [12, 13]. The HL shows a medium intensity band in the range of approximately 3140 cm^{-1} which is assigned to ν_{OH} of carboxylic acid group. On complexes this band was not detected.

The IR spectra of sodium salt of HL^1 show bands at 1589 cm^{-1}(s) and 1402 cm^{-1}(s), assigned to carboxyl group's antisymmerty stretch vibration $\nu_{as}(COO^-)$ and symmetry stretch vibration $\nu_s(COO^-)$. The IR spectra of complexes(**1**) shows bands at 1565 cm^{-1}(s) assigned to $\nu_{as}(COO^-)$ with a shift of 24 cm^{-1} to the lower frequency region, which compared with sodium salt of HL^1; The band at 1448 cm^{-1}(s) is assigned to $\nu_s(COO^-)$ with a shift of 46 cm^{-1} to the higher frequency region, which still compared with sodium salt of HL^1. This suggests that the carboxyl oxygen atom is involved in coordination with Nd(III) ion. In addition, the $\Delta\nu = \nu_{as}(COO^-)$-$\nu_s(COO^-)$ values (about 117 cm^{-1}) of the complex is lower than that of the Na salt (187 cm^{-1}), which indicate that there are bidentate carboxylate groups in the complex [14]. The shift of complexes(**2**) and (**3**) was the same as complex(**1**).

The ligand exhibits one sharp band at 1627 cm^{-1} (HL^1) and 1622 cm^{-1}(HL^2) due to heterocyclic (C = N) stretching vibration. The band of complexes almost wasn't shifted. Unobvious shifts indicating that the heterocyclic nitrogen atom does not take part in the coordination. Compared with the ligand, peaks of ν(C-O-C) in complexes blue-shifted by 4 cm^{-1} – 8 cm^{-1}, which suggests that cyclic ether oxygen involves in this coordination [15]. Two medium intensity band at 782 cm^{-1}, 577 cm^{-1}(**1**); 782 cm^{-1}, 579 cm^{-1}(**2**); 781 cm^{-1}, 583 cm^{-1}(**3**) are assignable to bending vibration of coordination water. The absorption bands around 1493–1495 cm^{-1}($\nu_1(NO_3^-)$) and 1299–1315 cm^{-1}($\nu_4(NO_3^-)$) for complex, suggests that there are bidentate coordinated nitrate in the complexes. New peaks appearing at 510 cm^{-1} or so are assigned to ν(Nd-O), which further confirms the involvement of coordination of oxygen to Nd (III). It was observed that the characteristic absorption peaks of the free nitrates are at about 1384 cm^{-1}.

Thermogravimetric analysis (TGA)

The thermal decomposition of the three complexes was studied using the TG-technique. The experiment was performed under a dynamic air atmosphere in temperature range from 30°C to 800°C at a heating rate of 10°C min^{-1}. It can be found that the thermal behaviors of the three complexes are quite similar. We can see that the decomposition temperature of the complex lower than its melting point. The TG-DTG curves of complex(**1**) are shown in Fig. 2. According to the curves, the first weight loss of 5.50% corresponding to the departure of the crystal water (calculated 5.98%) occurred in stages beginning at 50°C and finishing at about 147°C. The second weight loss of 6.50% corresponding to the departure of the coordination water (calculated 5.98%) occurred in the range of 148–175°C. Degradation of the pyrimidine was observed in the range of 176–248°C, corresponding to the weight loss of 13.02% (calculated 13.12%). Degradation of the norcantharidin acylamide acid as a residue was observed in the range of 249 –252°C, corresponding to the weight loss of 30.02% (calculated 30.39%). After that, the complex gave an endothermic peak at around 253–497°C corresponding to the weight loss of 9.48% (calculated 10.29%), and 498–675°C corresponding to the weight loss of 9.20% (calculated 10.29%), which indicates the thermal decomposition of free

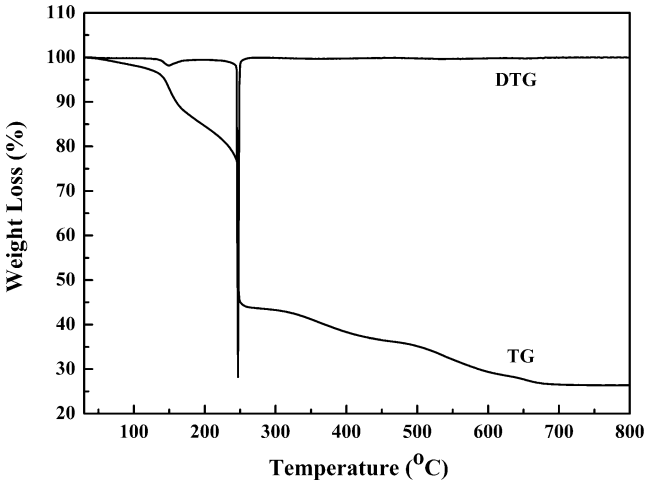

Fig. 2 The TG-DTG curves of the $[Nd(L^1)(NO_3)(H_2O)_2]\cdot NO_3\cdot 2H_2O$(**1**)

nitrate and coordinated nitrate, respectively. Beyond the range of 676 °C, the weight is constancy, 26.50% of the initial mass of the samples was left as a residue of Nd_2O_3 (calculated 27.90%). The results are in accordance with the composition of the complexes as determined by elemental analyses.

On the basis of above evidence and analyses, the suggested structure of the complexes is shown in Fig. 3.

DNA binding and cleavage studies

Fluorescence spectroscopic studies

The interaction mechanism of compounds with DNA can be studied by fluorescence spectra. When the compounds combine with DNA, their emission spectra and lifetime of excited states will change because the environment of the compounds varies. Therefore, the change of the fluorescence spectra indicate that the compounds can combine with DNA in a certain form. It is reported that if the emission of the compounds decreases obviously with the amount of DNA increasing, the compounds interact with DNA by intercalation fully [16] or partially [17].

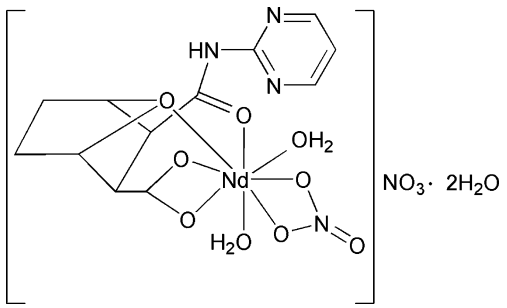

Fig. 3 The suggested structure of the $[Nd(L^1)(NO_3)(H_2O)_2]\cdot NO_3\cdot 2H_2O$(**1**)

The reductions in the emission intensity of the three complexes with ct-DNA concentration increasing are shown in Fig. 4. All the samples were excited at 280 nm, and the three complexes emit luminescence in the Tris-HCl buffer at ambient temperature, with a maximum emission wavelength at 363 nm (**1**) Fig. 4(a), 361 nm (**2**) Fig. 4(b) and 344 nm (**3**) Fig. 4(c), respectively. According to the Stern-Volmer equation [18]: $I_0/I=1+ K_{sv}$ [Q], where I_0 and I represent the fluorescence intensities in the absence and presence of DNA, respectively. [Q] is the concentration of DNA. The K_{sv} values for complex (**1**), (**2**) and (**3**) are $3.8\times10^4 L\cdot mol^{-1}$, $1.8\times10^4 L\cdot mol^{-1}$ and $4.0\times10^3 L\cdot mol^{-1}$, respectively. The dramatic change in the luminescence intensity of the complexes in presence of DNA strongly supports that the complexes bind to double-stranded DNA by intercalation. The stacking of the complexes with the base pairs of DNA leads to the transformation of electron and energy from the aromatic ring to the base pairs [19]. It can be found that reduction of the luminescence intensity of complex (**1**) and (**2**) was more than that of (**3**). This may be due to the L^1 and L^2 containing the pyrimidine and pyridine respectively, which can form hydrogen bonds with base pairs of DNA. As a result, the stacking of the heterocycle with base pairs of the DNA was enhanced.

The DNA-binding modes of three complexes were further monitored by a fluorescent EB displacement assay. It is well known that EB can emit intense fluorescence in the presence of DNA, due to its strong intercalation between DNA base pairs. It was previously reported that the enhanced fluorescence can be quenched by the addition of a second molecule [20]. The quenching extent of fluorescence is used to determine the extent of binding between the second molecule and DNA.

The intensity of emission band at 590 nm of the EB-DNA system was reduced with the increasing of the concentration of the complexes, which indicated that the complexes could displace EB from the EB-DNA system [21]. The quenching plots (insets in Fig. 5) illustrate that the quenching by the complexes are in good agreement with the linear Stern-Volmer equation. According to the classical Stern-Volmer equation [18]: $I_0/I=1+K_{sq}r$, where I_0 and I represent the fluorescence intensities in the absence and presence of the complex, respectively, r is the concentration ratio of the complex to DNA. K_{sq} is a linear Stern-Volmer quenching constant. The K_{sq} value is obtained by the slope. The K_{sq} values for complexes (**1**), (**2**) and (**3**) are 3.3(±0.21), 1.7(±0.19) and 0.9(±0.04), respectively. The data suggest that the binding ability of complex(**1**) with DNA is the strongest, followed by (**2**), and (**3**) which have the moderate intensity [22]. But the ligand (HL) can not quench the emission intensities of EB-DNA system obviously. It indicates that complex could bond to DNA more easily than HL, for there are several approximates planar six-membered

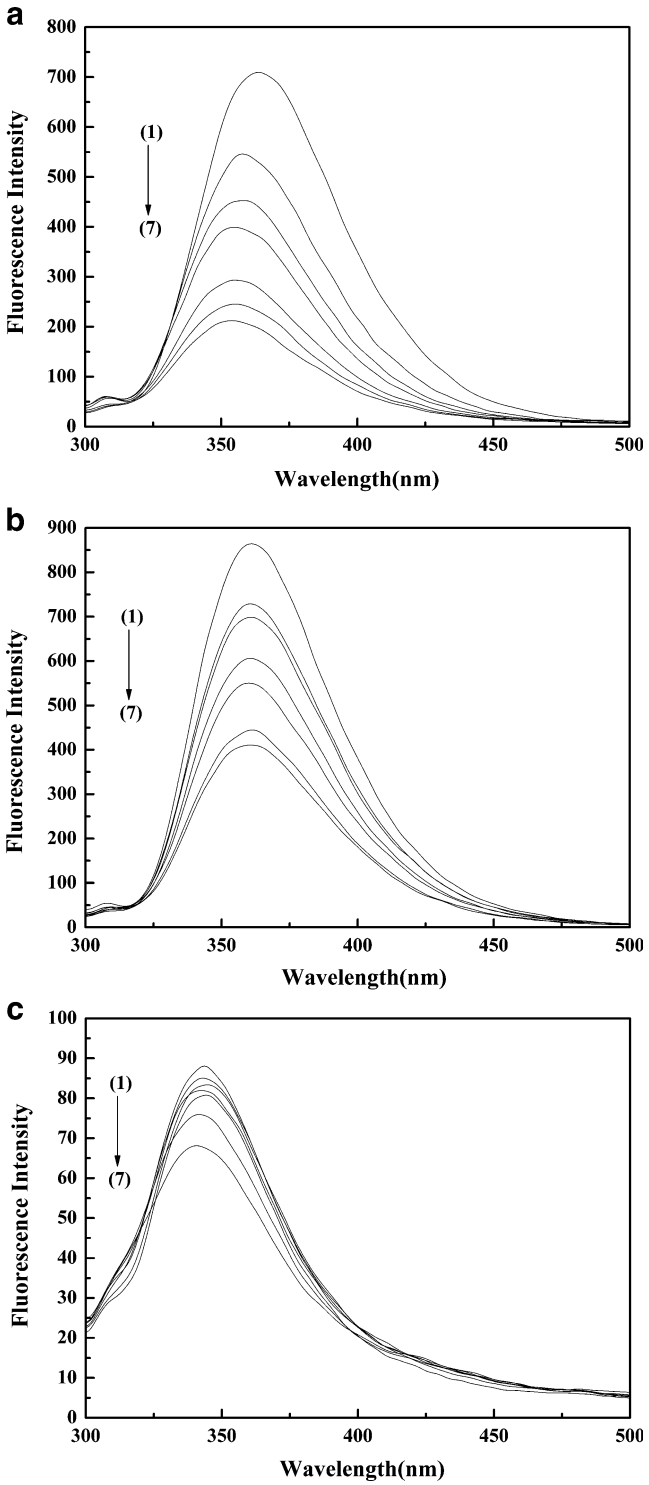

Fig. 4 Fluorescence spectra of the combination complex(**1**) (a), complex(**2**) (b) and complex(**3**) (c) in the absence and presence of increasing amounts DNA, λ_{ex}=280 nm, λ_{em}=300-500 nm. Arrows show the intensity changes upon increasing concentration of the DNA. [complex]=20 μmol·L^{-1}, [DNA]/10^{-5} mol·L^{-1}: (1): 0; (2): 0.9; (3): 1.8; (4): 2.7; (5): 3.6; (6): 4.5; (7): 5.4

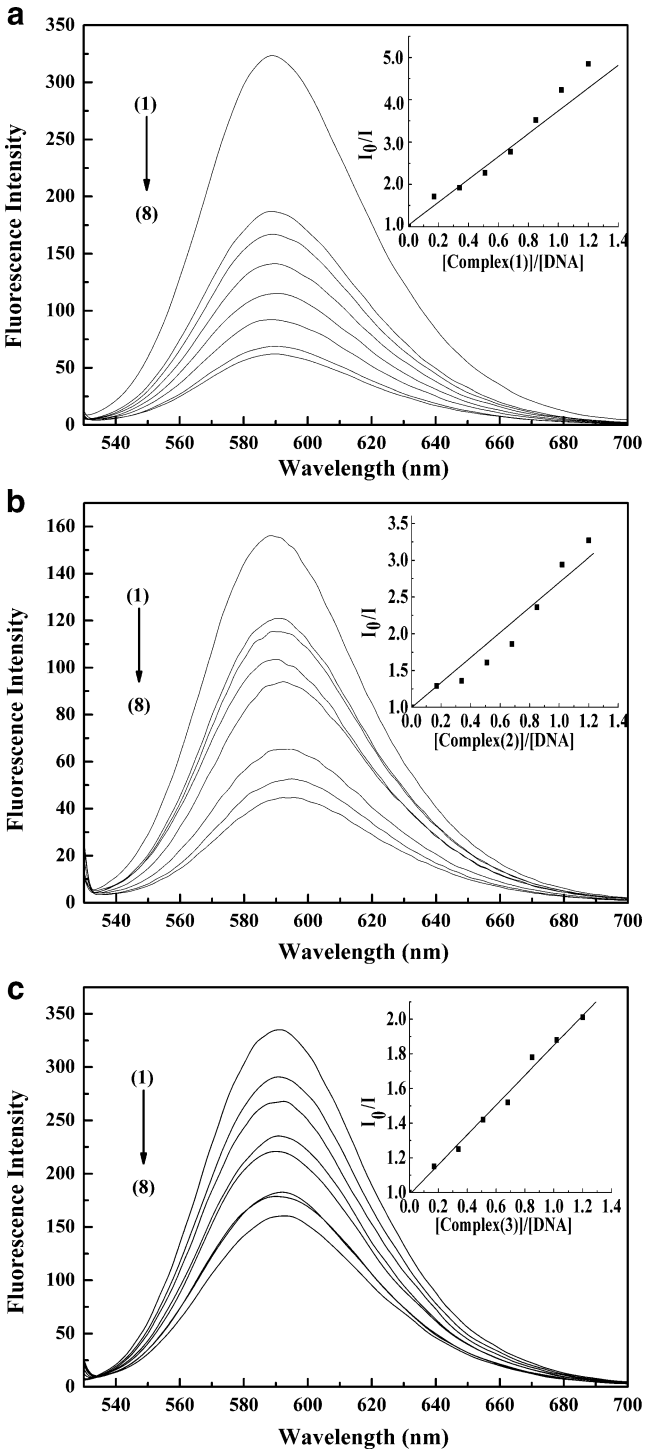

Fig. 5 Fluorescence spectra of the combination of EB and DNA in the absence and presence of increasing amounts of complex(**1**) (a), complex(**2**) (b) and complex(**3**) (c). λ_{ex}=525 nm, λ_{em}=530–700 nm. Arrows show the intensity changes upon increasing concentration of the complex. The illustrations are Stern–Volmer quenching curves. [EB]=50 μmol·L^{-1}; [DNA]=74 μmol·L^{-1}. (1) r=0; (2) r=0.17; (3) r=0.34; (4) r=0.51; (5) r=0.68; (6) r=0.85; (7) r =1.02; (8) r =1.20. r = [complex]/ [DNA]

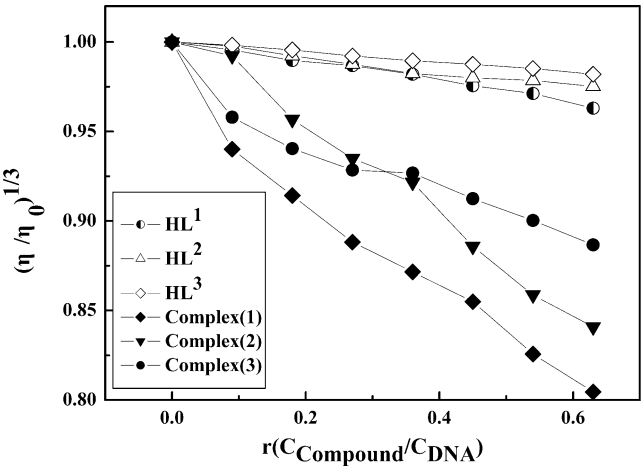

Fig. 6 Effect of increasing amounts of compounds on the relative viscosities of ct-DNA at 30 . [DNA] $=3.74\times10^{-4}$mol·L^{-1}, r = [compound]/ [DNA]. (1): r=0; (2): r=0.09; (3): r=0.18; (4): r=0.27; (5): r=0.36; (6): r=0.45; (7): r=0.54; (8): r=0.63

rings and seven-membered rings and flat NO_3^- in the complexes. As a result, the complexes could intercalate DNA and squeeze EB from DNA double helix more easily.

Viscosity study

As a means for further clarifying the binding of the compounds with DNA, viscosity measurements were carried out on ct-DNA by varying the concentration of the added compounds. Hydrodynamic measurements which are sensitive to length increase (for example, viscosity, sedimentation) are regarded as the least ambiguous and the most critical tests of binding in solution in the absence of crystallographic structure data [23]. A classical intercalative mode causes a significant increase in viscosity of DNA solution due to increase in separation of base pairs at intercalation sites and hence an increase in overall DNA length. In contrast, a partial, no-classical intercalation of compounds could bend (or kink) the DNA helix, reducing its effective length and, concomitantly, its viscosity [24].

As shown in Fig. 6, the effects of the HL and three complexes on the viscosity of ct-DNA at 30.0°C were investigated. The results reveal that the presence of the compounds decreases the relative viscosity of DNA and the decrease in the presence of the complexes is more than in presence of HL. This may be contributed to that Nd(III in complexes can further bond with the phosphate groups of DNA backbone[25]. The complexes decrease the relative viscosity of DNA, which was proposed to be bound to DNA by partial intercalation and lead to bends or kinks in the DNA. At the same time, the decrease degrees of DNA viscosity for complex(**1**) are more than that for complex(**2**) and complex (**3**), indicating that the complex containing pyrimidine is of higher binding affinity to DNA than other complexes.

Fluorescent titration experiment and viscosity measurement suggest that the complexes may bind to DNA by partial intercalation. The binding ability with DNA decreased in following order: complex(**1**), complex(**2**), and complex(**3**).

Gel eletrophoresis studies

The cleavage reaction on plasmid DNA can be monitored by agarose gel electrophoresis. When circular plasmid DNA is subjected to electrophoresis, relatively fast migrations will be observed for the intact supercoil form (FormI). If scission occurs on one strand (nicking), the supercoil will partial relax to generate a slower-moving open circular form (Form II) [26].

Figure 7 shows the electrophoretograms applying to the interaction of pBR322 plasmid DNA with HL^1 and complex. Initially, in the untreated pBR322 plasmid DNA (lane 1), the band corresponding to FormI was observed. Complex(**1**) (400μmol·L^{-1}, Fig. 7(b)) and complex(**2**) (400μmol·L^{-1}, Fig. 7(c)) can cleave the supercoiled plasmid DNA (FormI)

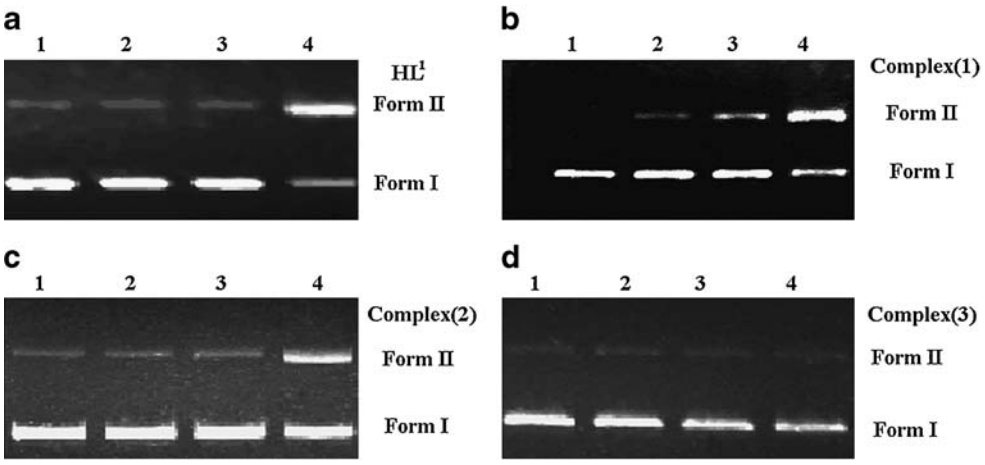

Fig. 7 Electrophoretic separation of pBR322 DNA induced by HL^1 (a), complex (**1**) (b), complex (**2**) (c) and complex (**3**) (d). [DNA] =3μg·mL^{-1}. lane 1: DNA alone; lane 2: DNA + compound (100μmol·L^{-1},); lane 3: DNA + compound (200 μmol·L^{-1},), lane 4: DNA + compound (400μmol·L^{-1},)

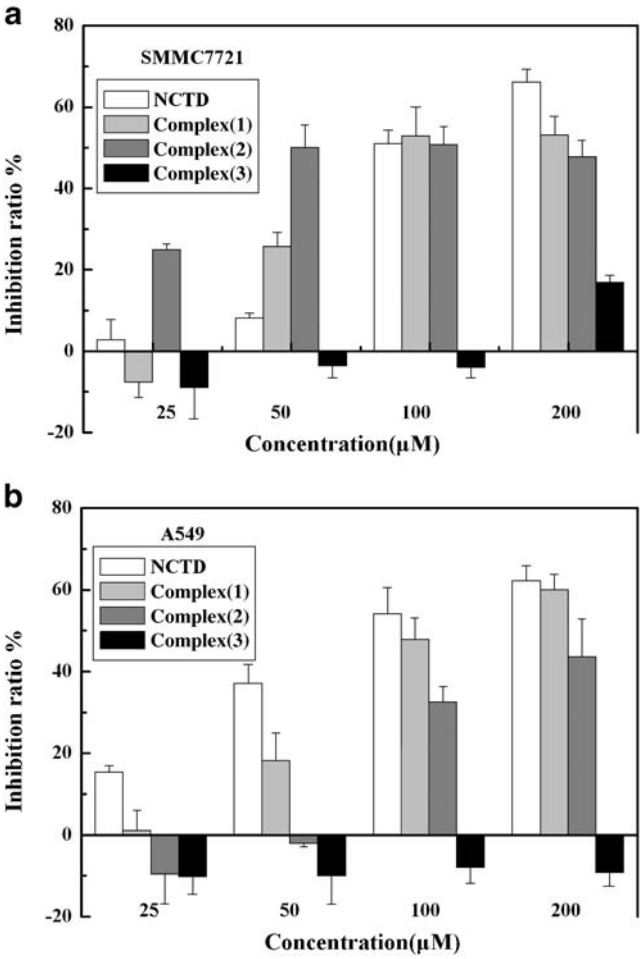

Fig. 8 Effect of NCTD and the complexes at different concentrations for 72 h on the proliferation of tumor cell. All assays were performed in triplicate for three independent experiments. (a): SMMC7721; (b):A549

to partial nicked circular DNA (FormII) while complex(**3**) (Fig. 7(d)). cannot cleave the supercoiled plasmid DNA. The cleavage ability of complex(**1**) is stronger than that of HL^1 (Fig. 7(a)). Complex(**1**) and complex(**2**) are believed to form monofunctional adducts with Guanine. The monofunctional adducts could close to form initially bifunctional interstrand GC adducts that can evolve into interstrand GG adducts. When bifunctional interstrand adducts is formed, complex(**1**) and complex(**2**), planar complexes containing nitrogen heterocycle will be positioned along the helix axis so that they will push apart adjacent base pairs [27]. All these results are well consistent with spectroscopic and viscosity measurement.

Antiproliferative activity evaluation

As shown in Fig. 8, the antiproliferative activity of the compounds at the given concentration against human hepatoma cells (SMMC7721, Fig. 8(a)) and human lung cancer cells (A549, Fig. 8(b)) in vitro viability was exhibited in a dose-dependent manner. As shown in Fig. 8(a), at lower doses (50 $\mu mol \cdot L^{-1}$), inhibition rates of complex(**1**) (25.6±3.7%) and complex(**2**) (50.1±5.5%) are much higher than that of NCTD (8.2±1.1%) against SMMC7721 cell lines. The complex(**2**) possesses strong antiproliferative effect toward SMMC7721 cell lines, but at higher doses (50–200 $\mu mol \cdot L^{-1}$), the antiproliferative activity did not increased. For A549 cell lines, all the complexes at the given concentration significantly decreased the tumor cell viability in a dose-dependent manner. As shown in Fig. 8(b), at the tested doses (0-200 $\mu mol \cdot L^{-1}$), inhibition rates of the complex(**1**) are much higher than that of complex (**2**) and (**3**) against A549 cell lines. At 200 $\mu mol \cdot L^{-1}$, inhibition rate of complex (**1**) (60.0±3.8%) is much higher than that of complex(**2**) (43.6±9.3%) and complex(**3**) (−9.3±3.2%) against A549 cell lines. In the range of tested concentration, complex(**3**) almost showed no antiproliferative activity against the tested cell lines.

The concentration of the compounds for 50% inhibition (IC_{50}) on the SMMC7721 and A549 cell lines were determined and the results were summarized in Fig. 9. As shown in Fig. 9, the test of antiproliferation activity indicates that complex(**1**) has strong antiproliferative ability against the SMMC7721 (IC_{50}=131.7±23.4 $\mu mol \cdot L^{-1}$) and A549 (IC_{50}=128.4±19.9 $\mu mol \cdot L^{-1}$) cell lines. The inhibition rates of complex(**2**) (IC_{50}=86.3±11.3 $\mu mol \cdot L^{-1}$) are much higher than that of NCTD (IC_{50}=115.5±9.5 $\mu mol \cdot L^{-1}$), HL^2 (111.0±5.7 $\mu mol \cdot L^{-1}$) and other complexes against SMMC7721 cell lines. Generally, the complex containing heterocycle exhibited higher antiproliferative effect than the complex containing benzene ring. But there is no clearly direct correlation between interaction of the complexes with DNA and antiprolififerative activity of the complexes.

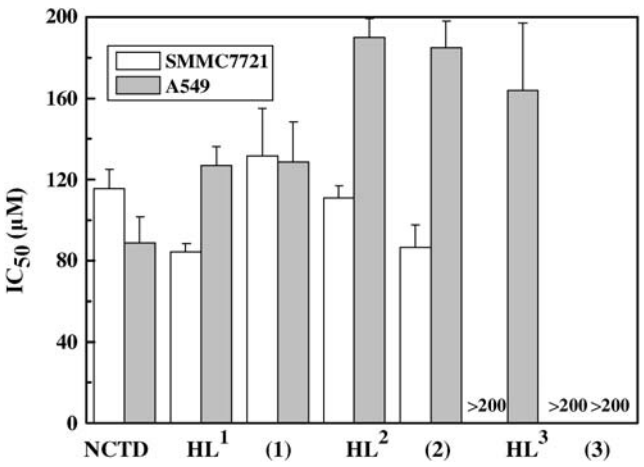

Fig. 9 72-h IC_{50} values of test compounds in SMMC7721 and A549 cells lines. Data represent mean ± SD. All assays were performed in triplicate for three independent experiments

Conclusions

Three novel Nd(III) complexes $[Nd(L)(NO_3)(H_2O)_2]\cdot NO_3\cdot 2H_2O$, (HL = norcantharidin acylamide acid) were synthesized and characterized. The complexes can bind to DNA by partial intercalation binding modes. Noticeably, the complex (**1**) and (**2**) have been found that they not only more easily bind to ct-DNA in comparison with (**3**) and HL but also can cleave pBR 322 DNA at physiological pH and temperature. These observations suggest that Nd(III) ion and the heterocycle attached to the norcantharidin can enhance the binding extent of the complexes with DNA. Generally, the complexes containing heterocycle exhibite higher antiproliferative effect than the complexes containing benzene ring. The results show that complex(**1**) have stronger antiproliferative activity to the human lung cancer cells (A549). Complex(**2**) containing N-pyridine norcantharidin acylamide acid exhibites higher antiproliferative effect against human hepatoma cells (SMMC7721), especially at the low concentration, and it seems to be well suited for further work aiming at the development of new anticancer agents.

Acknowledgment This work received financial support from the Natural Science Foundation of Zhejiang Province, China (Grant No. Y407301).

References

1. McCluskey A, Bowyer MC, Collins E, Sim ATR, Sakoff JA, Baldwin ML (2000) Anhydride modified cantharidin analogues: synthesis, inhibition of protein phosphatases 1 and 2A and anticancer activity. Bioorg Med Chem Lett 10:1687–1690. doi:10.1016/S0960-894X(00)00323-1
2. Wang GS (1989) Medical uses of mylabris in ancient China and recent studies. J. Ethnopharmacol. 26:147–162. doi:10.1016/0378-8741(89)90062-7
3. Hill TA, Stewart SG, Ackland SP, Gilbert J, Sauer B, Sakoff JA, McCluskey A (2007) Norcantharimides, synthesis and anticancer activity: synthesis of new norcantharidin analogues and their anticancer evaluation. Bioorg Med Chem 15:6126–6134. doi:10.1016/j.bmc.2007.06.034
4. Hill TA, Stewart SG, Sauer B, Gilbert J, Ackland SP, Sakoff JA, McCluskey A (2007) Heterocyclic substituted cantharidin and norcantharidin analogues—synthesis, protein phosphatase (1 and 2A) inhibition, and anti-cancer activity. Bioorg Med Chem Lett 17:3392–3397
5. Kostova I, Ilia Manolov, Spiro Konstantinov, Karaivanova M (1999) Synthesis, physicochemical characterisation and cytotoxic screening of new complexes of cerium, lanthanum and neodymium with Warfarin and Coumachlor sodium salts. Eur. J. Med. Chem 34:63–68. doi:10.1016/S0223-5234(99)80041-5
6. Li TR, Yang ZY, Wang BD, Qin DD (2008) Synthesis, characterization, antioxidant activity and DNA-binding studies of two rare earth(III) complexes with naringenin-2-hydroxy benzoyl hydrazone ligand. Eur. J. Med. Chem 43:1688–1695. doi:10.1016/j.ejmech.2007.10.006
7. Ho YP, To KKW, Yeung SCFA, Wang XN, Lin G, Han X (2001) Potential new antitumor agents from an innovative combination of demethylcantharidin, a modified traditional Chinese medicine, with a platinum moiety. J Med Chem 44:2065–2068. doi:10.1021/jm000476t
8. Yang H, Guo W, Xu B, Li M, Cui J (2007) Anticancer activity and mechanisms of norcantharidin-Nd3II on hepatoma. Anticancer Drugs 18:1133–1137
9. Stewart SG, Hill TA, Gilbert J, Ackland SP, Sakoff JA, McCluskey A (2007) Synthesis and biological evaluation of norcantharidin analogues: Towards PP1 selectivity. Bioorg Med Chem 15:7301–7310. doi:10.1016/j.bmc.2007.08.028
10. Zheng XL, Sun HX, Liu XL, Chen YX, Qian BC (2004) Astilbic acid induced COLO 205 cell apoptosis by regulating Bcl-2 and Bax expression and activating caspase-3. Acta Pharmacol Sin 25:1090–1095
11. Geary WJ (1971) The use of conductivity measurements in organic solvents for the characterisation of coordination compounds. Coord Chem Rev 7:81–122. doi:10.1016/S0010-8545(00)80009-0
12. Xu ZD, Liu H, Xiao SL, Yang M, Bu XH (2002) Synthesis, crystal structure, antitumor activity and DNA-binding study on the Mn(II) complex of 2*H*-5-hydroxy-1,2,5 -oxadiazo[3,4-f] 1,10-phenanthroline. J Inorg Biochem 90:79–84. doi:10.1016/S0162-0134(02)00416-6
13. Wang Y, Wang Y, Yang ZY (2007) Synthesis, characterization and DNA-binding studies of 2-carboxybenzaldehydeisonicotinoylhydrazone and its La(III), Sm(III) and Eu(III) complexes. Spectrochim Acta A Mol Biomol Spectrosc 66:329–334. doi:10.1016/j.saa.2006.02.062
14. Nakamoto K (1978) Infrared and raman spectra of inorganic and coordination compounds. Wiley-Interscience, New York
15. Yin FL, Zou JJ, Xu L, Wang X, Li RC (2005) Synthesis, characterization and antitumor activity of Lanthanum (III) complex with demethylcantharidate. J Rare Earths 23:596–599
16. Chaires JB, Dattagupta N, Crothers DM (1982) Studies on interaction of anthracycline antibiotics and deoxyribonucleic acid: equilibrium binding studies on the interaction of daunomycin with deoxyribonucleic acid. Biochem 21:3933–3940. doi:10.1021/bi00260a005
17. Mesmaeker AKD, Orellana G, Barton JK, Turro NJ (1990) Ligand-dependent interaction of Ruthenium (II) polypyridyl complexes with DNA and probed by emission spectroscopy. Photochem. Photobiol. 52:461–472. doi:10.1111/j.1751-1097.1990.tb01787.x
18. Lakowicz JR, Webber G (1973) Quenching of fluorescence by oxygen. Probe for structural fluctuations in macromolecules. Biochem 12:4161–4170. doi:10.1021/bi00745a020
19. Wu JZ, Yuan L, Wu JF (2005) Synthesis and DNA binding of μ-[2,9-bis(2-imidazo[4,5-f] [1,10] phenanthroline)-1,10-phenanthroline]bis[1,10-phenanthrolinecopper (II)]. J Inorg Biochem 99:2211–2216. doi:10.1016/j.jinorgbio.2005.08.002
20. Barton JK, Raphael AL (1984) Photoactivated stereospecific cleavage of double- helical DNA by cobalt(III) complexes. J. Am. Chem. Soc 106:2466–2468. doi:10.1021/ja00320a058
21. Zeng YB, Yang N, Liu WS, Tang N (2003) Synthesis, characterization and DNA-binding properties of La(III) complex of chrysin. J. Inorg. Biochem 97:258–264. doi:10.1016/S0162-0134(03)00313-1
22. Liu J, Zhang TX, Lu TB, Qu LH, Zhou H, Zhang QL, Ji LN (2002) DNA-binding and cleavage studies of macrocyclic copper (II) complexes. J. Inorg. Biochem 91:269–276. doi:10.1016/S0162-0134(02)00441-5
23. Baguley BC, Bret ML (1984) Quenching of DNA-ethidium fluorescence by amsacrine and other antitumor agents: a possible electron-transfer effect. Biochem 23:937–943. doi:10.1021/bi00300a022
24. Satyanarayana S, Dabrowiak JC, Chaires JB (1993) Tris(phenanthroline)ruthenium(II) enantiomer interactions with DNA: Mode

and specificity of binding. Biochem 32:2573–2584. doi:10.1021/bi00061a015
25. M. Komiyama, N. Takeda, H. Shigekawa, (1999), Hydrolysis of DNA and RND by lanthanide ions: mechanistic studies leading to new applications, *Chem Comm*. 1443-1451.
26. Kelly TM, Tossi AB, McConnell DJ, Strekas TC (1985) A study of the interactions of some polypyridylruthenium(II) complexes with DNA using fluorescence spectroscopy, topoisomerisation and thermal denaturation. Nucleic Acids Res 13:6017–6034. doi:10.1093/nar/13.17.6017
27. Chowdhury MA, Huq F, Abdullah A (2005) Synthesis, characterization and binding with DNA of four planaramineplatinum(II) complexes of the forms: *trans*-PtL_2Cl_2 and $[PtL_3Cl]Cl$, where L = 3-hydroxypyridine, 4-hydroxypyridine and imidazo(1,2-α)pyridine. J. Inorg. Biochem 99:1098–1112. doi:10.1016/j.jinorgbio.2005.02.002